

Ab initio study of semiconducting carbon nanotubes adsorbed on the Si(100) surface: diameter- and registration-dependent atomic configurations and electronic properties

Salvador Barraza-Lopez^{1,3}, Peter M. Albrecht^{2,3}, Nichols A. Romero^{1,4}, and Karl Hess^{1,2,3}

¹ Loomis Laboratory of Physics

² Department of Electrical and Computer Engineering

³ Beckman Institute for Advanced Science and Technology

⁴ Materials Research Laboratory and Materials Computation Center

University of Illinois. Urbana, IL, 61801, USA

(Dated: February 8, 2020)

We present a theoretical study within density functional theory in the local density approximation of semiconducting carbon nanotubes adsorbed on the unpassivated Si(100) surface. We find that the interaction between the nanotube and silicon surface results in significant atomic re-arrangement of the surface atoms. Since the spatial configuration of the surface dimers determines to a great extent the electronic properties of the surface, our first-principles calculations indicate a tendency towards metallicity for the semiconducting tube-Si(100) surface system. We confirm this for nanotubes of different diameters and chiral angles, and find the effect to be independent of the orientation of the nanotubes on the surface.

PACS numbers: 68.35.-p, 68.43.-h, 68.43.Bc, 73.22.-f

I. INTRODUCTION

First-principles studies illustrating the effect of technologically relevant semiconductor surfaces such as InAs,¹ GaAs² and Si(100)^{3,4,5} on the electronic properties of single walled carbon nanotubes (SWNTs) have been published recently. In the case of Si(100), the study was centered on determining the lowest-energy structural configuration and modifications to the electronic structure of an individual (6,6) (metallic) SWNT on this surface. This calculation was performed both for a nanotube in the proximity of a clean or selectively hydrogen-terminated⁵ Si(100) surface where the nanotube axis is parallel to the trench between adjacent Si dimer rows. Remarkably, there have been no studies of this system for semiconducting tubes, in different geometrical configurations, nor on the dependence of the properties of the hybrid system against nanotube diameter. These are relevant issues to be addressed as experimental techniques which minimize surface contamination for depositing SWNTs onto doped Si(100) and other semiconductor surfaces in ultra-high vacuum (UHV) at room temperature have been reported.^{6,7,8} As contaminant-free atomistic manipulation becomes more feasible, the promise of molecular systems with tunable electronic and mechanical properties becomes a reality. It is clear that near-term applications for carbon nanotubes in electronic devices would benefit from their integration with conventional semiconductor platforms such as Si or GaAs. In this direction, rectifying carbon nanotube-Si heterojunction arrays have been demonstrated,⁹ and semiconductor heterostructures of GaAs/AlAs and (Ga,Mn)As have been used as contacts for individual SWNTs.¹⁰ Recent experiments¹¹ showing the existence of two preferential directions for the growth of SWNT on Si indicate that there is a non-negligible interaction between the SWNT and its substrate. One relevant issue which remains to

be addressed is the nature of the mechanical and electronic properties of the hybrid semiconductor-nanotube interfaces.

In this work, we explore the interaction between the unpassivated Si(100) surface and semiconducting carbon nanotubes using density functional theory (DFT) when the nanotubes are in orientations parallel or perpendicular relative to the Si dimer row direction. We highlight the effect of electrostatic interactions on the atomic configuration of the surface caused by the proximity of the SWNT and ultimately on the electronic properties of the hybrid Si-SWNT system. In Section II, we discuss the theoretical approximations employed and the structural configurations considered in this study. The resulting atomic configurations of the combined Si(100)-SWNT system and its electronic properties are presented in Section III. Our conclusions and future work are described in section IV.

II. METHODS

We have performed density functional theory¹² (DFT) calculations of semiconducting nanotubes with varying diameters (5-15 Å) on the clean Si(100) surface, and complemented those with additional calculations on metallic nanotubes of comparable diameter. Our calculations in the local density approximation¹³ (LDA) were performed with the SIESTA code.¹⁴ The exchange-correlation potential employed is the one parameterized by Perdew-Zunger,¹⁵ based on the Ceperley-Alder data.¹⁶ Core electrons are replaced by norm-conserving Troullier-Martin pseudopotentials.¹⁷ For the greater variational freedom, a double- ζ basis set for s and p orbitals, and a single- ζ basis set for d orbitals was constructed using the prescription of Junquera *et al.*¹⁸ To ensure the transferability of our basis, the basis set parameters were optimized by means

TABLE I: Lattice constants obtained with our bases, which exemplify the transferability of our basis set.

Element	Theoretical estimate (Å)	This work (Å)
C (Diamond)	3.570 (Ref. 21)	3.486
C (Graphene)	<i>a</i> 2.450 (Ref. 22)	<i>a</i> 2.448
	<i>c</i> 6.500 (Ref. 22)	<i>c</i> 6.516
Si (Diamond)	5.430 (Ref. 21)	5.401

of the simplex algorithm¹⁹ on graphite and diamond for the carbon basis and on diamond for the silicon basis. An equivalent plane-wave cutoff of 200 Ry was used to calculate the charge density on the real-space grid. To obtain the mechanical properties of these systems, we used a Monkhorst-Pack grid²⁰ with a single k -point, and increased the sampling in k -space with a $4 \times 4 \times 1$ grid prior to obtaining band structures and densities of states.

With our bases, we obtained lattice parameters for bulk silicon and carbon in the diamond and graphite structures. As shown in Table I, the lattice constants we use in our calculations compare well with previous theoretical estimates. We use the $p(2 \times 2)$ surface reconstruction for our semiconducting tubes as well as for the (8,8) and (10,10) metallic SWNTs. We calculate the structural and electronic properties of a (9,3) metallic SWNT in the LDA to compare against the previously studied GGA result for the (6,6) SWNT^{3,4,5}, and we used a $c(4 \times 2)$ reconstruction of the Si(100) surface for this case.²⁴ The surfaces constructed have six Si monolayers (the bottom-most H-passivated), with dimensions $3L \times 2L$ or $3L \times 3L$, depending on the length of the unit cell of the nanotube ($L = 7.639$ Å).

Since we are interested in trends that could complement both experimental work in this area and published theoretical results on metallic SWNTs on this surface we choose SWNTs satisfying the following criteria:

1. They should be semiconducting.
2. Their diameter should be of the order of 10 Å.
3. They should be commensurate with the underlying surface.

Table II lists the nanotubes studied in this work. In bold we indicate the diameter and length of the (6,6) nanotube extensively studied by Orellana and coworkers. We study the metallic (9,3) nanotube to assess the effect of the local exchange-correlation potential employed as well as the tube's chirality in comparison with previous work.^{3,4,5} We mention that while (n,n) (metallic) SWNTs happen to be commensurate to within 3% with the underlying Si(100) surface, the shortest commensurate semiconducting SWNT would be 15.391 Å long. This is one of the reasons why no theoretical work on semiconducting nanotubes has been carried out to date. The large unit cell sizes involved in calculations have deterred researchers from performing DFT calculations. The relevant geometric parameters such as the distance between the SWNT

TABLE II: Carbon nanotubes with diameter ~ 10 Å and length of their unit cell commensurate to within 2% with respect to the unit cell of the Si(100) surface. In bold, the respective values for the (6,6) SWNT studied before^{3,4,5} (commensurate to within 3%).

Nanotube	Diameter (Å)	Length of unit cell (Å)
(6,2)	5.657	15.391
(8,4)	8.302	11.294
(12,4)	11.314	15.391
(9,3)	8.486	15.391
(6,6)	8.153	2.465(3%)

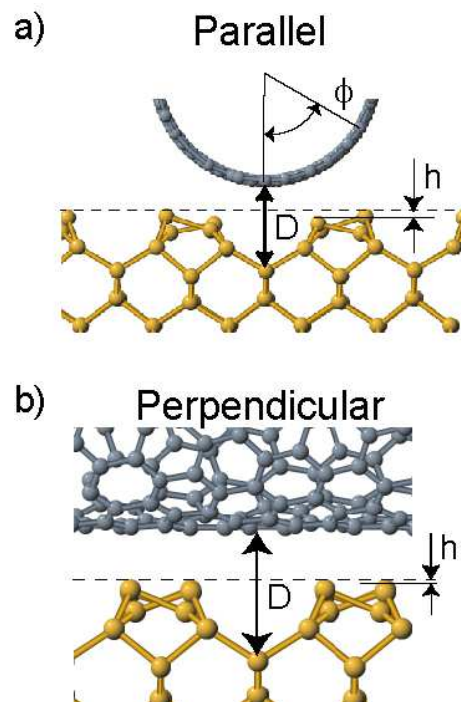


FIG. 1: SWNT on the Si(100) surface. We simulated semiconducting SWNTs deposited in two configurations: a) parallel, over the dimer trench and b) perpendicular to the Si(100) dimer trench. D is the lowest-energy distance from the bottom of the SWNT to the bottom of the Si dimer trench, h indicates the distance Si atoms closest to the SWNT retract and ϕ is the angle of rotation of the SWNT about its axis.

and the dimer trench D , the distance of the Si atoms closest to the SWNT retract h and the angle of rotation ϕ of the nanotube about its axis are schematically shown in Fig. 1.

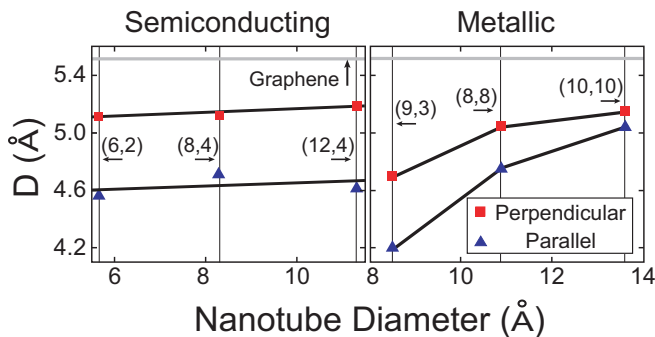


FIG. 2: (Color online) The distance D from the bottom of the dimer trench to the lowest carbon atom as a function of nanotube diameter, for fixed ϕ . Semiconducting tubes above the dimer trench in this diameter range will be closer to the underlying surface by about 0.5 \AA in comparison with tubes in the perpendicular configuration. Notice a more pronounced dependence for metallic SWNTs. Solid lines are drawn as a guide to the eye to facilitate the visualization of trends.

III. RESULTS

A. Optimized atomic and angular configurations

1. Distance from the nanotubes to the bottom of the dimer trench and amount of reconfiguration of the Si(100) surface

The diameter of the nanotube as well as its electronic character (metallic, semiconducting) are the deciding factors on the relative distance between the nanotube and the surface: As the nanotube diameter increases, the distance D from the SWNTs to the bottom of the dimer trench also increases asymptotically towards 5.52 \AA , which would be the separation between a graphene sheet and the Si(100) surface, as can be seen in Fig. 2. Here, we also calculated the optimal energetics versus distance D for (8,8) and (10,10) SWNTs for a fixed angle ϕ in order to distinguish trends between semiconducting and metallic SWNTs. Conjugate-gradient atomic relaxation was carried out with a single k -point. Due to the system size (with unit cells ranging from 296 to 512 atoms), this choice is sufficient to converge the total energy, and to obtain the system's optimal structural configuration.

We found a stronger diameter dependence on the distance for metallic SWNTs. For the semiconducting nanotubes studied the diameter dependence is not as marked. Yet, the tubes in the perpendicular configuration are positioned about 0.5 \AA farther from the surface compared to the parallel configuration, in accordance with experimental observation.²⁵

Figure 3 shows the average distance $\langle h \rangle$ that the silicon surface dimers retract due to the proximity of the SWNT. It shows that the Si(100) surface in the proximity of the SWNT undergoes a striking atomic reconstruction. We indicate, for comparison, that after atomic relaxation

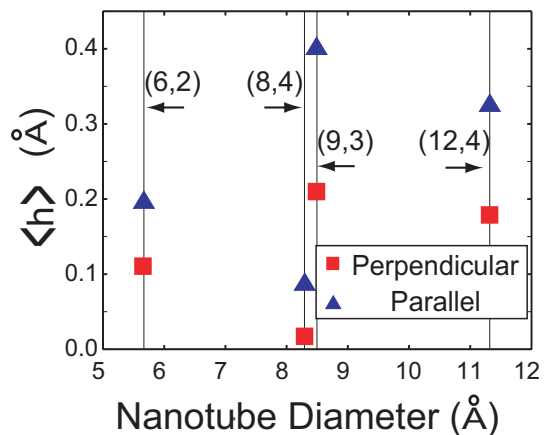


FIG. 3: (Color online) Average distance $\langle h \rangle$ that the uppermost Si dimer atoms retract as the SWNT is brought to proximity as a function of nanotube diameter. As the electronic properties of the Si(100) surface are closely related to the atomic configuration, the atomic rearrangement has consequences on the electronic structure of the Si-SWNT system. In contrast, the SWNTs in proximity remain very stiff, with almost unnoticeable atomic rearrangement.

our nanotubes undergo almost no structural change but remain very stiff. This suggests that the SWNT is physisorbed on the highly-reactive Si(100) rather being covalent bonded to it.

2. Optimal energy as the nanotube is rotated about its axis

Once the optimal height was found for a fixed angle, we rotated the SWNT about its axis to obtain the change in the system's energy versus ϕ . The results are shown in Fig. 4, where two sets with three curves each, can be discerned. The lower set of curves belongs to tubes in the parallel configuration, and the three upper curves on the figure to nanotubes in the perpendicular configuration. For our chiral tubes, the range of angles is given by $(0, 2\pi \times \text{GCD}(m, n))$, where $\text{GCD}(m, n)$ is the greatest common divisor of m and n . This range gives the maximum angular freedom that the nanotubes will have before the position of their carbon atoms become periodic. The tubes parallel to the trench are always lower in energy as compared to the ones in the perpendicular configuration, although due to the small energy difference, configurations with an arbitrary angle to the dimer trench are observed in experiments.²⁵ The (6,2) nanotube with the smallest studied diameter shows the more pronounced oscillations, due to the fact that it is closest to the Si surface and therefore it can greatly modify its energy as C and Si atoms are brought closer to each other as a result of the tube's rotation about its own axis. This is evidence of registration in this hybrid system.

In the previously studied case (Refs. 3,4,5) the highly symmetric atomic arrangement of the achiral (6,6)

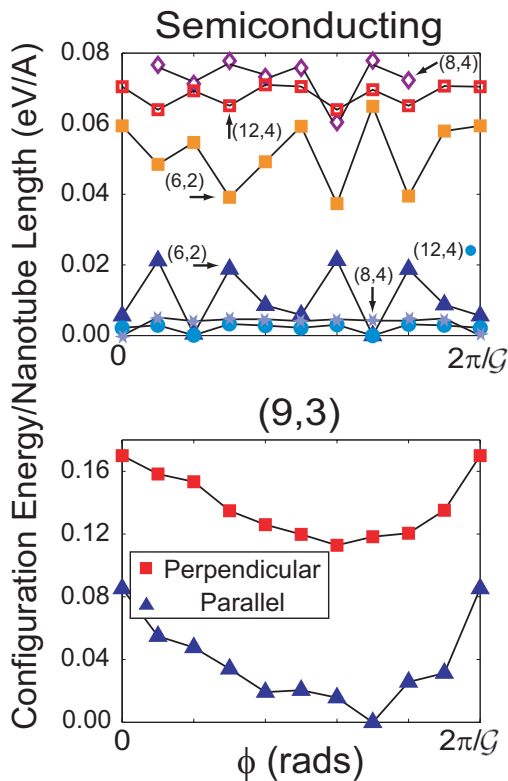


FIG. 4: (Color online) Angular dependence with respect to tube axis of the configuration energy, at fixed height ($\mathcal{G} \equiv \text{GCD}(m, n)$). Lower energies occur for tubes parallel to the trench and the energy dependence is more marked as the nanotube diameter is decreased (refer to the horizontal axis in Fig. 3 to visualize the SWNTs diameters). The metallic tube has an energy dependence twice as big as the semiconducting tubes.

SWNT with respect to the underlying Si atoms results in optimal angular configurations with varying D , and they found two minimum energy configurations. Nevertheless in a more general setting, chirality precludes highly symmetric configurations from occurring: the relative position of C atoms closest to the surface with respect to surface Si atoms becomes a complicated function of the chiral angle. In Fig. 4 we observe a small dependence (of the order of hundreds of meV) on energy against the tube's angle of rotation ϕ .

It is also apparent from Fig. 4 that the metallic nanotube displays an energy dependence on the angle of rotation twice as large as the semiconducting SWNTs. This is consistent with the fact that metallic tubes stay closer to the surface in comparison to semiconducting nanotubes of the same diameter. This could also be influenced by the different surface reconstruction we employed.

B. *Ab initio* electronic properties of the hybrid Si(100)-SWNT system

We show in Fig. 5 the band structures we obtained by first increasing the k -sampling in the plane defining the surface by using a $4 \times 4 \times 1$ Monkhorst-Pack mesh. In all plots the SWNT axis is parallel to the $\Gamma - J'$ direction. In the first column, we show results for nanotubes 10 \AA away from the surface. The gray lines show the band structure of the Si(100) surface, and the black lines depict bands from the SWNTs. Dotted horizontal lines show the respective Fermi levels when the SWNT and the surface do not interact. We notice a consistent Fermi level offset of about $\sim 0.5 \text{ eV}$ for semiconducting SWNTs, and half this value for the metallic SWNT. The resulting *ab initio* band structure and DOS for the parallel and perpendicular configurations can be seen in the second and third columns, respectively. In some of the plots we observe the occurrence of small gaps. Surface-SWNT interactions lift the degeneracy of bands in turn increasing the spectral density around the Fermi level.

The most salient feature from Fig. 5 is that, according to DFT, the hybrid Si(100)-SWNT system becomes metallic even with a *semiconducting* SWNT in proximity. This metallicity occurs according to our calculations, independently of the relative orientation of the semiconducting nanotubes with respect to the bottom of the Si(100) dimer trench. Therefore, semiconducting nanotubes in this diameter range adsorbed on this surface with *any* relative angle of their axes with respect to the direction defined by the bottom of the Si(100) dimer trench will create a conducting electronic channel.

We mention in passing that we are currently developing a tight-binding parametrization that will correct the electronic gap underestimation common in density functional theory and will allow us to perform a more precise electronic characterization of this system.

IV. CONCLUSIONS

We have studied semiconducting SWNTs adsorbed on the Si(100) surface. The proximity of the SWNTs alters the atomic positions of the first four monolayers on the Si(100) surface, and this effect is particularly pronounced for the first two monolayers. This leads to an interesting modification of the electronic properties of the hybrid system.

Semiconducting SWNTs of the diameter range studied are placed at an almost constant distance to the surface. Those tubes are 0.5 \AA closer to the surface when they are above and aligned with the trench between adjacent dimer rows, in comparison with any other configuration in which the trench and the tube axis do not align. We found a weak angular dependence on the configurational energy of the system, and we believe this dependence will be further lowered as the length of the nanotube's unit cell increases, due to the loss of symmetry in the relative

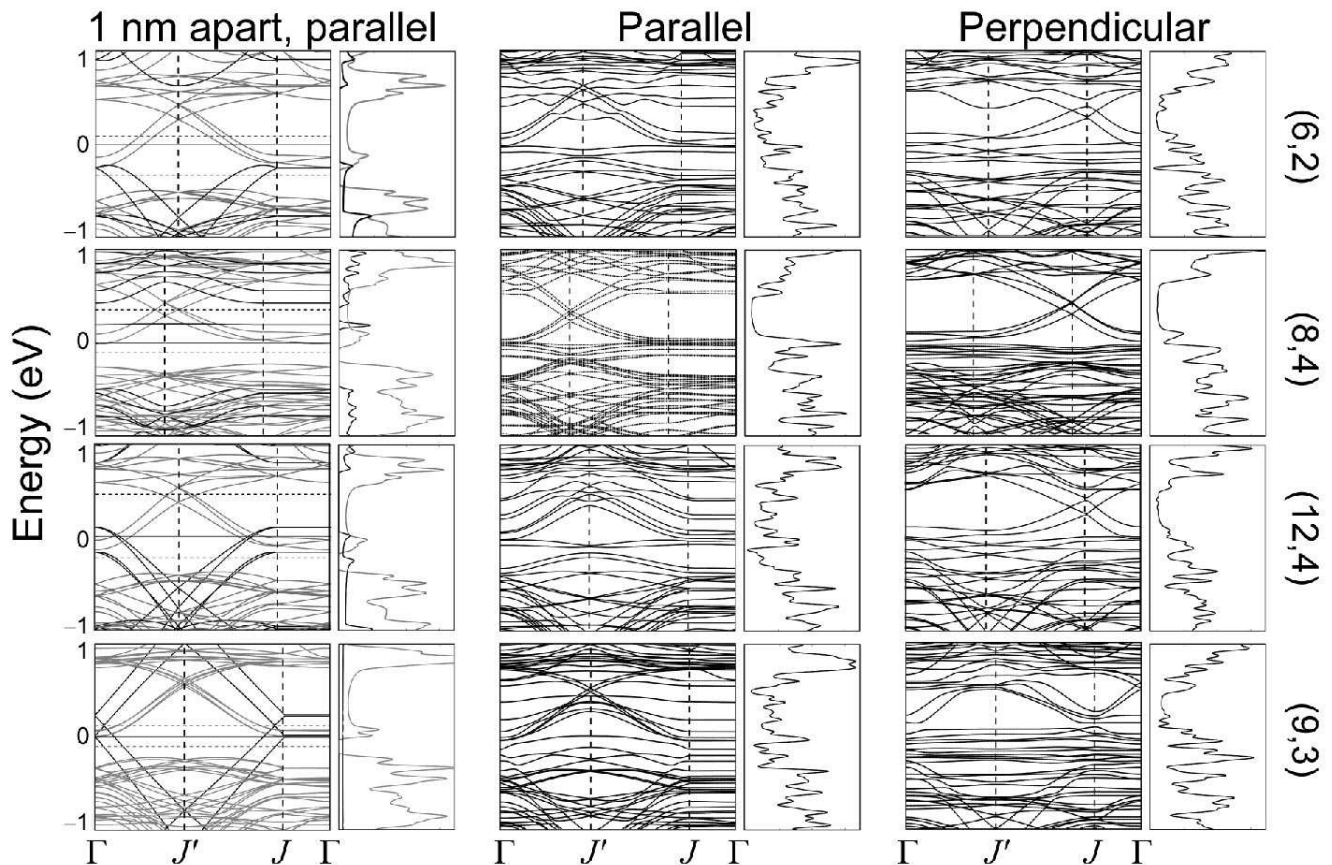


FIG. 5: *Ab initio* band structures and densities of states for SWNTs in different alignments with respect to the Si(100) surface. First column shows the band structures of subsystems when they are far from each other: Gray lines correspond to the Si(100) surface and black lines to the SWNTs. There is an ~ 0.5 eV Fermi level offset for the semiconducting SWNTs and a smaller offset for the metallic SWNT. Next columns show the band structure and DOS for SWNTs aligned on top of the dimer trench (parallel) and with its axis crossing the dimers in a perpendicular configuration (perpendicular), after atomic relaxation was performed. The *ab initio* results show metallicity for the hybrid system composed of semiconducting tubes and the Si(100) surface. The different positions for the J , J' points reflects the difference in size of the unit cells considered. We employed a 200K gaussian spreading to plot the DOS.

positions of the C atoms in the SWNT closest to the Si surface atoms. With the exception of two metallic (8,8) and (10,10) nanotubes, our SWNTs have lengths in their unit cell along the tube axis of at least six times of that studied by Orellana *et al.* For the (9,3) SWNT, we found in agreement with Refs. 3,4 that it stays metallic in either configuration, but the weak angular dependence tells us it will remain at an almost fixed height D , independent of its angular orientation. Our similar results show that the essential results are independent of the approximation employed for the exchange-correlation functional (LDA or GGA).

The electronic properties of these hybrid systems will vary in a qualitative way according to the relative orientation of the SWNT (parallel, perpendicular) with respect to the surface, but we find from our calculations that semiconducting tubes of the diameter studied here will become metallic in both studied configurations. We further believe this implies that those studied semiconduct-

ing SWNTs will be metallic in *any* surface configuration relative to the dimer trench.

We are currently developing a highly tuned tight-binding algorithm to explore the electronic properties of this system, as DFT underestimates the magnitude of the electronic band gap for Si. That will allow us to provide a more accurate description of the electronic properties of this system. Currently, experimental results on this system are starting to emerge.²⁵ We hope that the results provided in this paper motivate further experimental work in the area, as the properties described in here might be useful for electronic applications.

ACKNOWLEDGMENTS

G. Bauer and G. Lopez-Walle assisted during the early stages of this project. We thank R. M. Martin, N. Tayebi,

K. Ritter and H. Terrones for useful discussions. Calculations were performed on the CSE mac OS X Turing cluster, linux CEG cluster (U. Ravaioli, Z. Yang). This work was supported by National Computational Science Alliance under grant number DMR050032N (NCSA's IBM

pSeries 690 Cooper cluster) and the Office of Naval Research, grant N00014-98-1-0604. S. B.-L. acknowledges partial funding from CONACyT (Mexico), P.M.A. a NDSEG graduate fellowship and N.A.R. grants from NSF (DMR-0325939) and DoE (DEFG02-91ER45439).

-
- ¹ Y.-H. Kim, M. J. Leben, and S. B. Zhang, Phys. Rev. Lett. **92**, 176102 (2004).
- ² Y.-H. Kim, M. J. Heben, and S. B. Zhang (AIP conference proceedings, 2004), pp. 1031–1032, in *Physics of Semiconductors: 27th International conference on the Physics of Semiconductors*.
- ³ W. Orellana, R. H. Miwa, and A. Fazzio, Phys. Rev. Lett. **91**, 166802 (2003).
- ⁴ W. Orellana, R. H. Miwa, and A. Fazzio, Surf. Sci. **566-568**, 728 (2004).
- ⁵ R. H. Miwa, W. Orellana, and A. Fazzio, Appl. Phys. Lett. **86**, 213111 (2005).
- ⁶ P. M. Albrecht and J. W. Lyding, Appl. Phys. Lett. **83**, 5029 (2003).
- ⁷ P. M. Albrecht and J. W. Lyding (AIP conference proceedings, 2004), pp. 173–177, in *Electronic Properties of Synthetic Nanostructures*.
- ⁸ L. B. Ruppalt, P. M. Albrecht, and J. W. Lyding, J. Vac. Sci. Technol. B **22**, 1071 (2004).
- ⁹ M. Tzolov, B. Chang, A. Yin, D. Straus, and J. M. Xu, Phys. Rev. Lett. **92**, 075505 (2004).
- ¹⁰ A. Jensen, J. R. Hauptmann, J. Nygard, J. Sadowski, and P. E. Lindelof, Nano Lett. **4**, 349 (2004).
- ¹¹ M. Su, Y. Li, B. Maynor, A. Buldum, J. P. Lu, and J. Liu, J. Phys. Chem. B **104**, 6505 (2000).
- ¹² P. Hohenberg and W. Kohn, Phys. Rev. **136**, B864 (1964).
- ¹³ W. Kohn and L. J. Sham, Phys. Rev. **140**, A1133 (1965).
- ¹⁴ J. M. Soler, E. Artacho, J. D. Gale, A. Garcia, J. Junquera, P. Ordejon, and D. Sanchez-Portal, J. Phys.: Condens. Matter **14**, 2745 (2002).
- ¹⁵ J. P. Perdew and A. Zunger, Phys. Rev. B **23**, 5048 (1981).
- ¹⁶ D. M. Ceperley and B. J. Alder, Phys. Rev. Lett. **45**, 566 (1981).
- ¹⁷ N. Troullier and J. L. Martins, Phys. Rev. B **43**, 1993 (1991).
- ¹⁸ J. Junquera, O. Paz, D. Sanchez-Portal, and E. Artacho, Phys. Rev. B **64**, 235111 (2001).
- ¹⁹ W. H. Press, S. A. Teukolsky, W. T. Vetterling, and B. P. Flannery, *Numerical recipes in fortran 77*, vol. 1 of *Fortran Numerical Recipes* (Cambridge U. Press, 1992), 2nd ed.
- ²⁰ H. J. Monkhorst and J. D. Pack, Phys. Rev. B **13**, 5188 (1976).
- ²¹ N. W. Aschcroft and N. D. Mermin, *Solid State Physics* (Harcourt College Publishing, Fort Worth, 1976), p. 76.
- ²² K. R. Kganyago and P. E. Ngoepe, Phys. Rev. B **68**, 205111 (2003).
- ²³ R. Nicklow, N. Wakabayashi, and H. G. Smith, Phys. Rev. B **5**, 4951 (1972).
- ²⁴ S. B. Healy, C. Filippi, P. Kratzer, E. Penev, and M. Scheffler, Phys. Rev. Lett. **87**, 016105 (2001).
- ²⁵ P. M. Albrecht and J. W. Lyding, unpublished (2005).